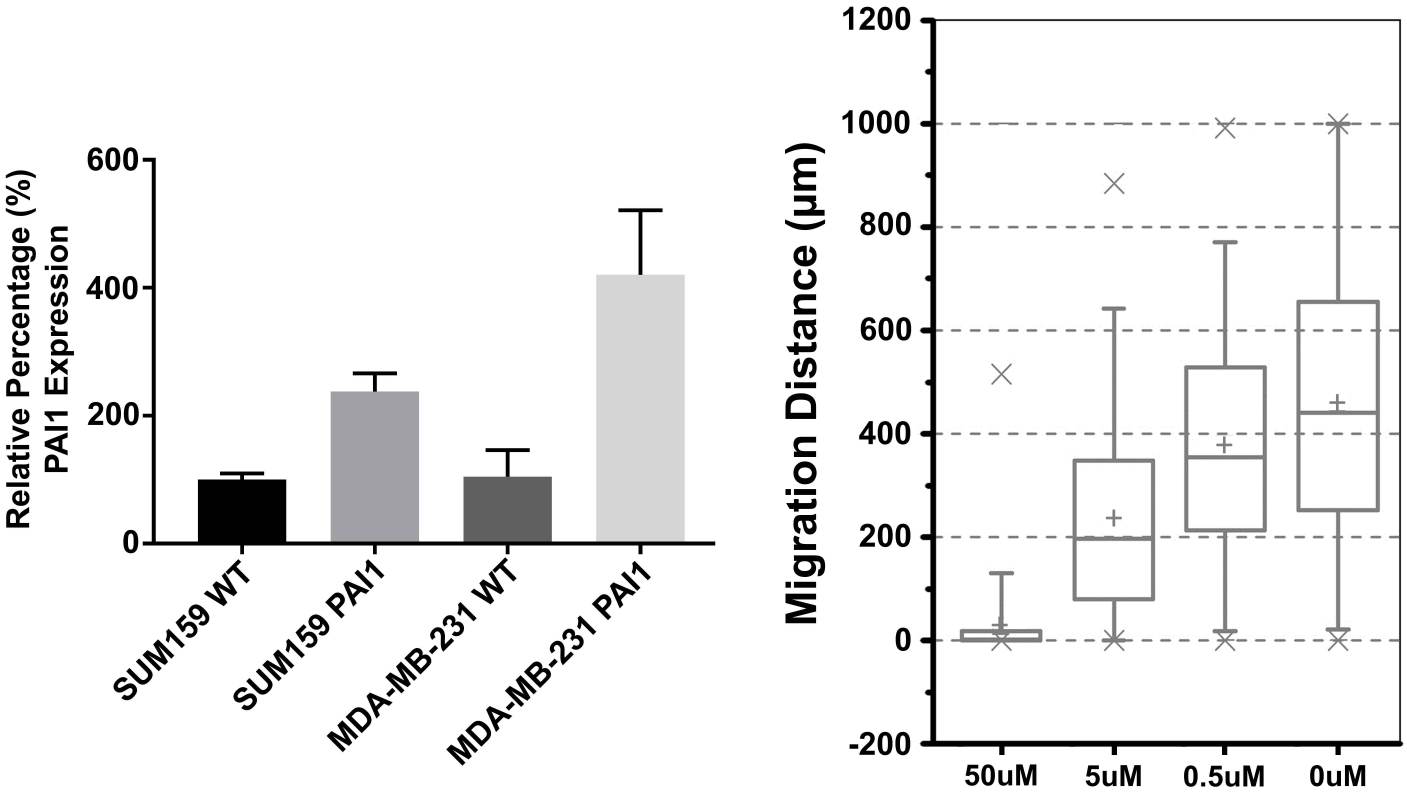

Supplemental Figure S1. Overexpression of PAI1 in SUM159 PAI1 and MDA-MB-231 PAI1 cells and effects of tiplaxtinin on cell migration. Left. qRT-PCR results demonstrate that PAI1 is overexpressed by > 2-fold in both MDA-MB-231 and SUM159 triple negative breast cancer cells. Graphs show mean + SD expression relative to WT cells. **Right.** Graph displays positions of individual cells and box plot and whiskers summaries for migration of SUM159 cells after 24 hours of treatment with different concentrations of the PAI1 inhibitor tiplaxtinin. Treatment with 50 µM tiplaxtinin was toxic to the cells, so we selected 5µM for the remainder of experiments. Graphs are depicted as described in the Materials and Methods. The “x” outside the box plot and whiskers indicate maximum and minimum of all the data.

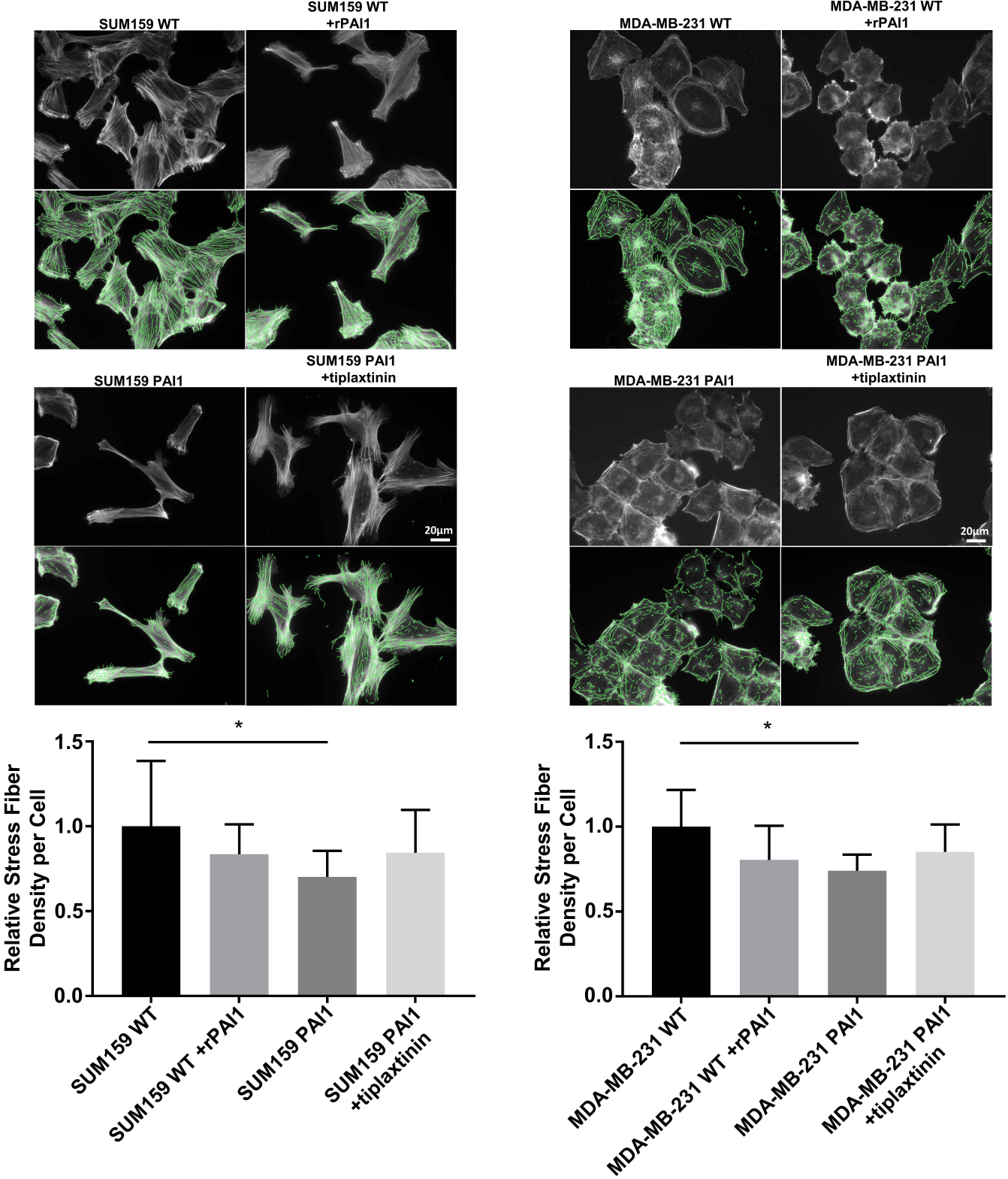

Supplemental Figure S2. PAI1 reduces stress fiber formation and inhibition partially recovers the phenotype. Representative images of stress fibers and stress fiber analysis (mean + SD) in SUM159 and MDA-MB-231 WT and PAI1 cells stained with phalloidin under baseline conditions or following treatment with rPAI1 (40 nM) or tiplaxtinin (5 µM) (n ≥ 10 images). We analyzed stress fibers with custom MATLAB code.

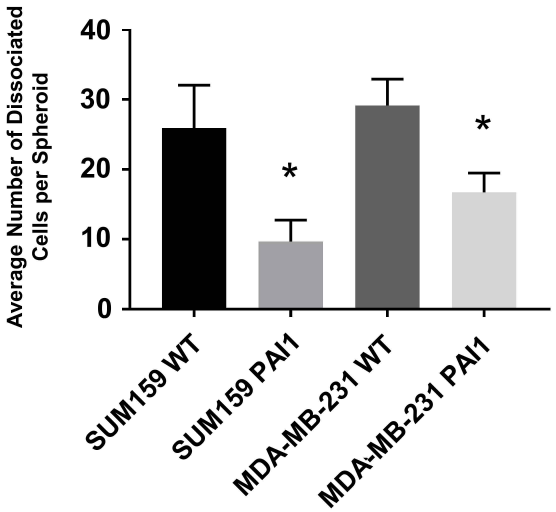

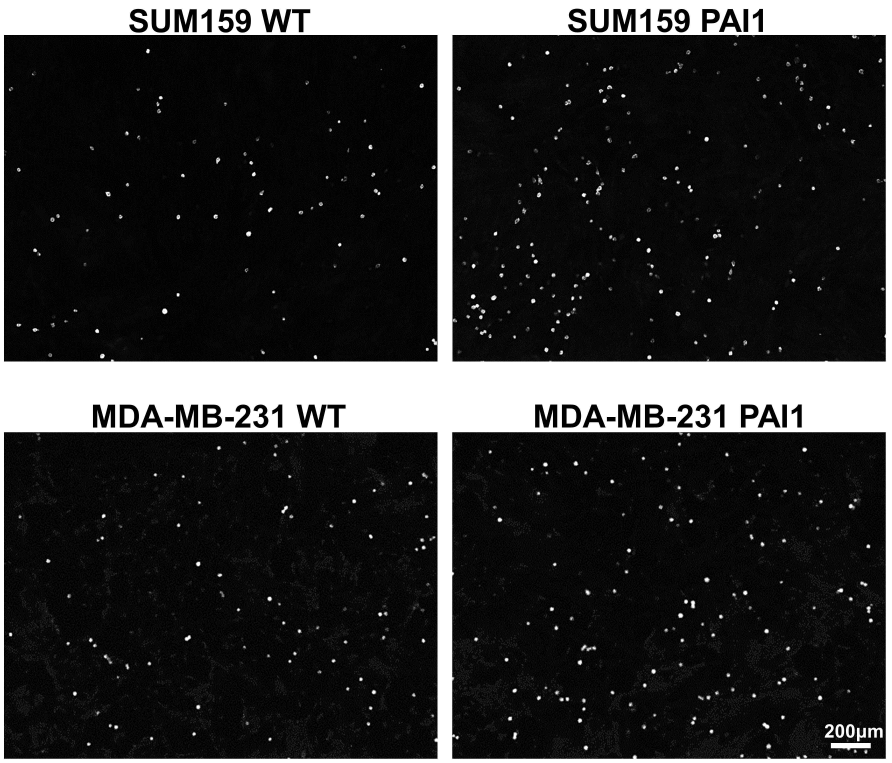

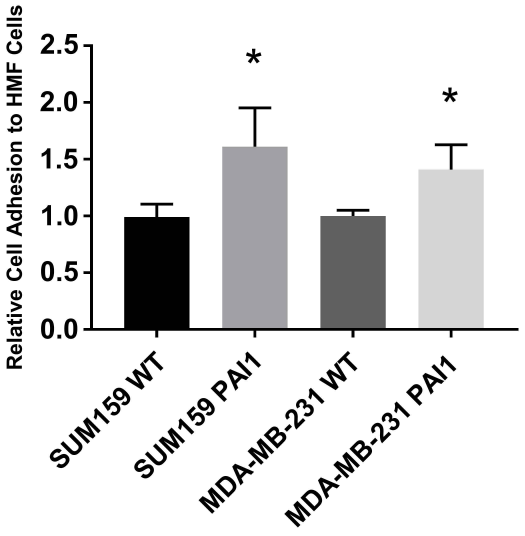

Supplemental Figure S3. PAI1 promotes adhesion. Top. Spheroids made of PAI1 cells and HMFs dissociate less than WT spheroids with HMFs. Graphs show mean number of cells detached from the spheroid after mechanical dissociation + SD (n = 9). * = $p < 0.05$. **Bottom.** PAI1 promotes adhesion to HMFs. Representative images of WT and PAI1 stably expressing cells attached to human mammary fibroblasts (HMFs). Graphs show mean number of cells attached to HMFs + SD (n = 15) relative to WT cells. * = $p < 0.05$.

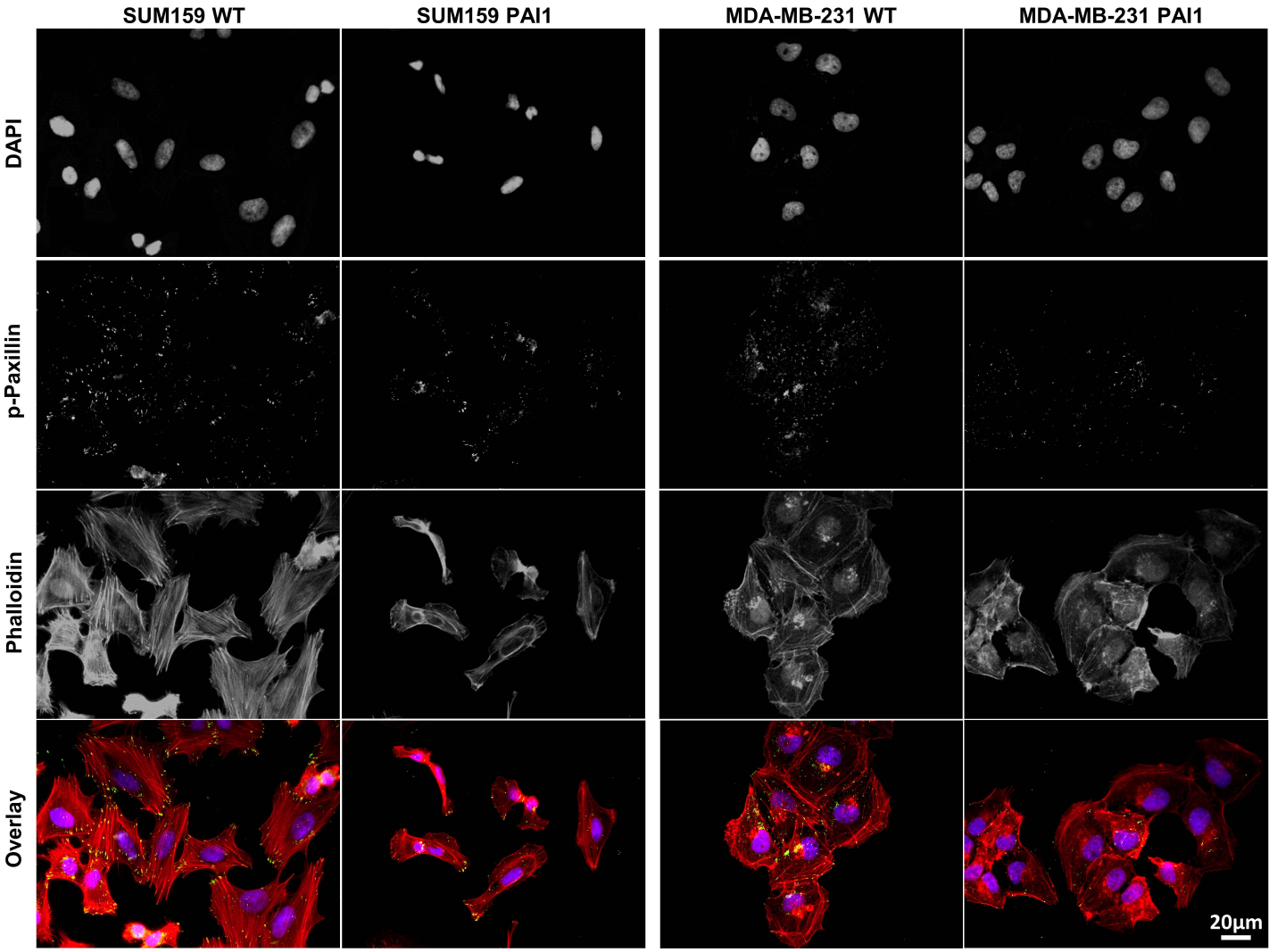

Supplemental Figure S4. PAI1 stimulates actin cytoskeleton reorganization and reduces focal adhesions. Representative overlaid images of immunofluorescence staining of phalloidin (red), DAPI (blue), and phospho-paxillin (green) of WT and PAI1 cells.

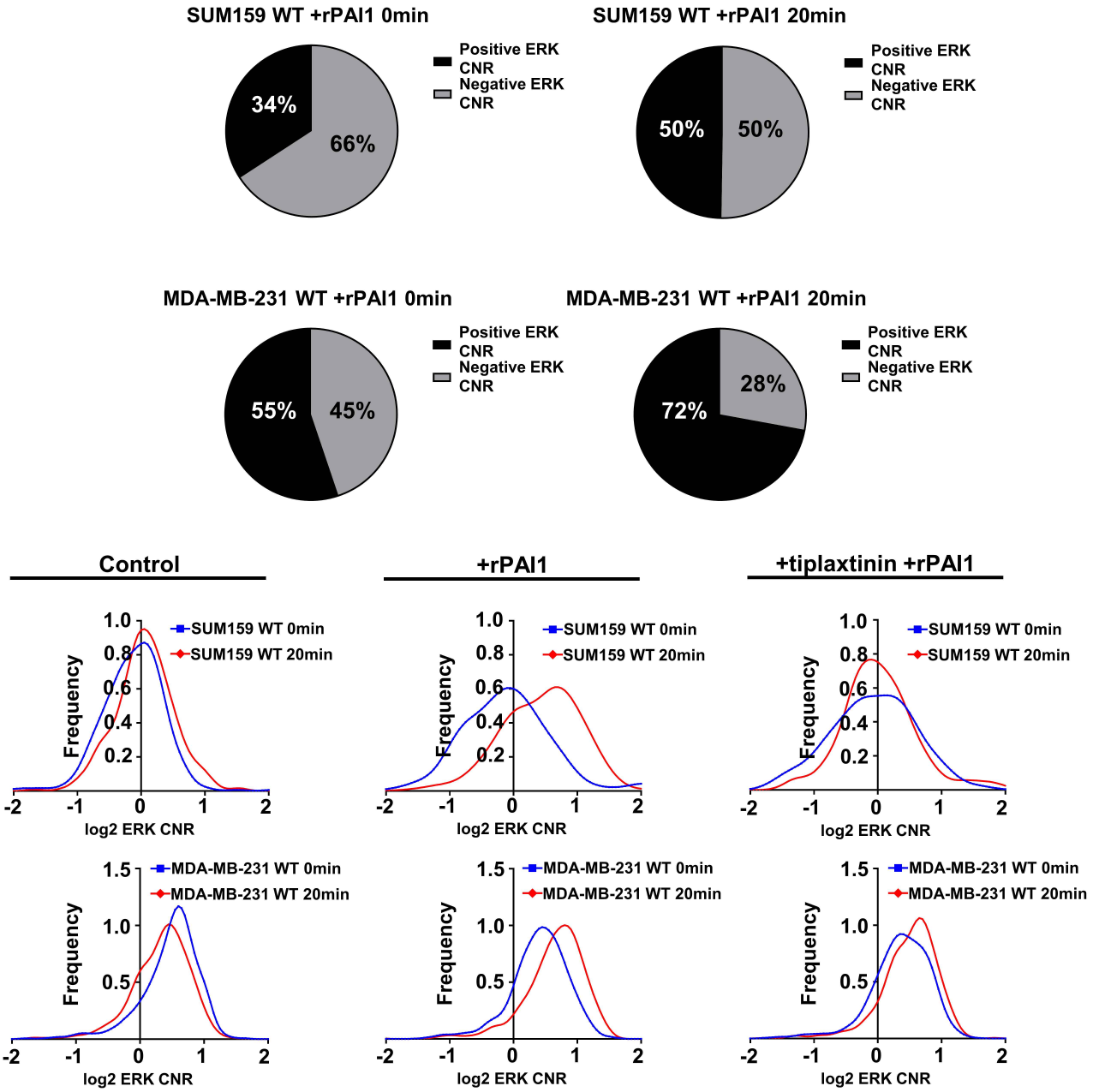

Supplemental Figure S5. rPAI1 activates ERK signaling. Top. Pie graphs showing percentages of positive (> 0) and negative (< 0) ERK KTR CNR values for both SUM159 and MDA-MB-231 WT cells at the initial timepoint and 20 minutes after addition of 40 nM rPAI1 shown in Figure 4. The increase in positive CNR values indicates activation of ERK kinase activity. **Bottom.** Frequency distribution of cytoplasmic-to-nuclear ratio (CNR) of SUM159 (n > 215 cells) and MDA-MB-231 (n > 400 cells) WT cells at the initial timepoint (0 mins) and 20 minutes after addition of rPAI1 (n = 1). A shift to the right demonstrates activation of ERK signaling.

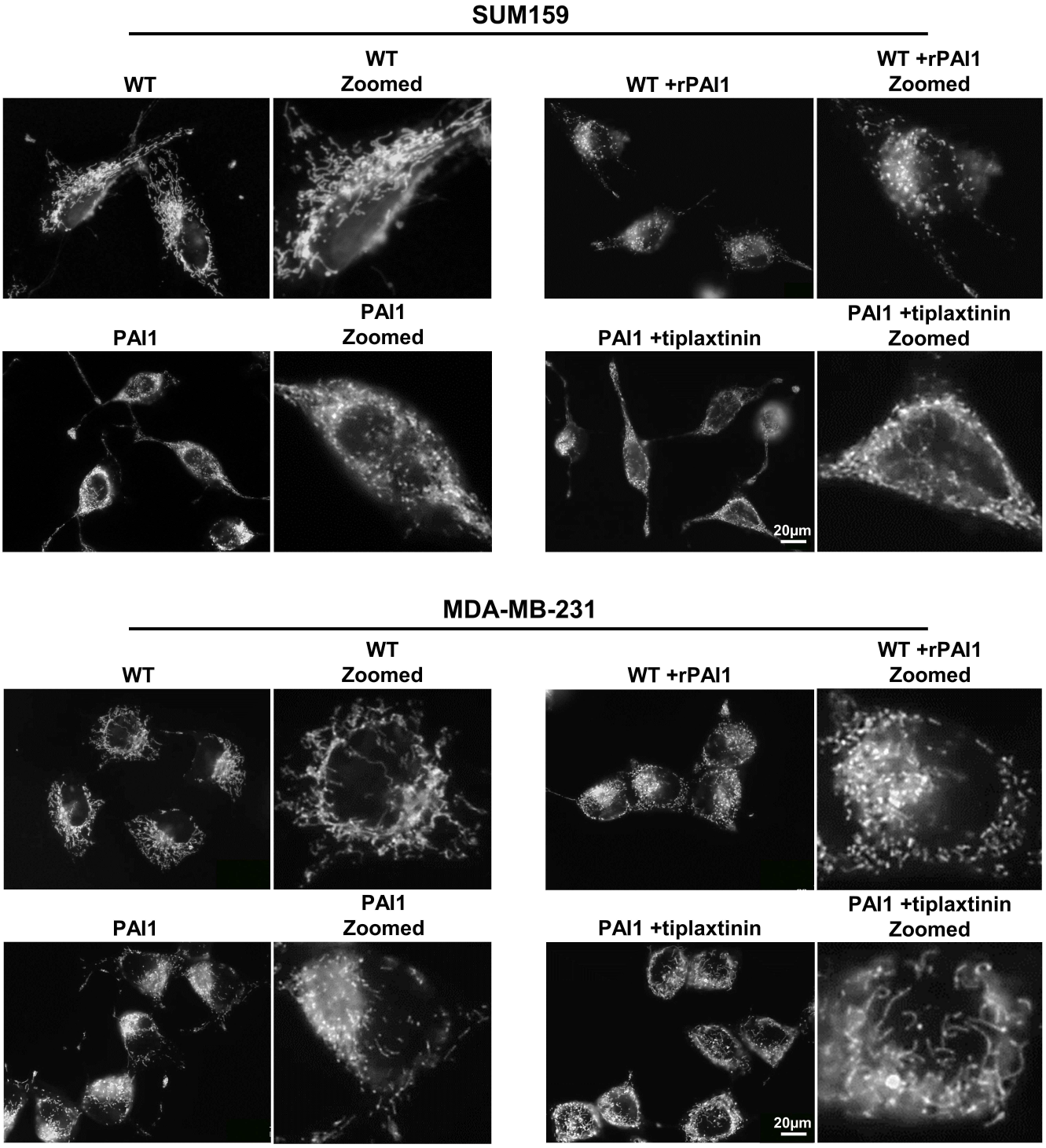

Supplemental Figure S6. PAI1 promotes fragmented mitochondrial morphology and inhibition partially recovers the phenotype. Representative images of mitochondria in SUM159 and MDA-MB-231 WT and PAI1 cells stained with MitoTracker Green under baseline conditions or following treatment with rPAI1 (40 nM) or tiplaxtinin (5 µM) for 24 hours.

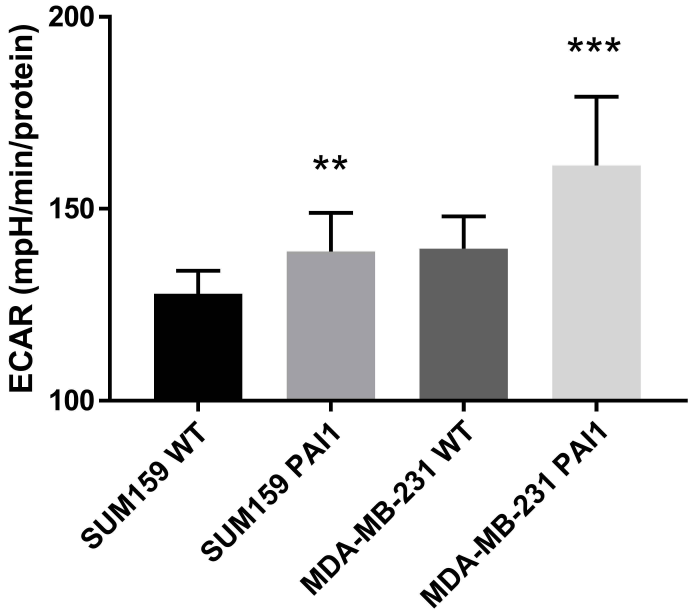

Supplemental Figure S7. PAI1 promotes glycolysis. Extracellular acidification rate (ECAR) was measured under basal conditions (n ≥ 14). Graph shows mean + SD. ** refers to $p < 0.01$. *** refers to $p < 0.001$.

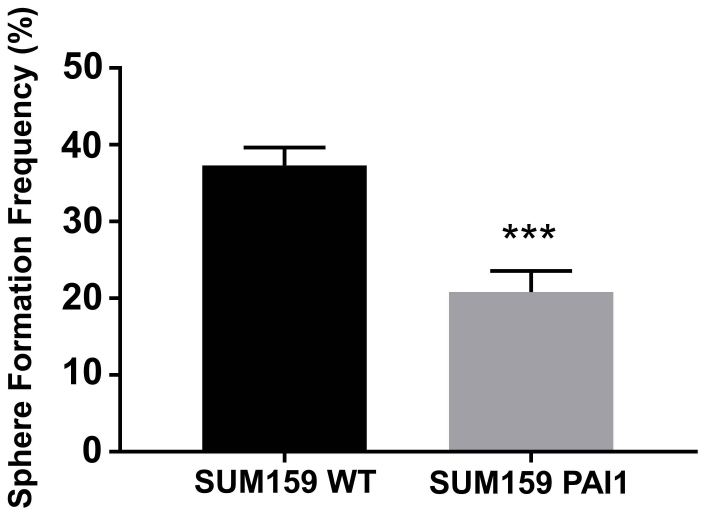

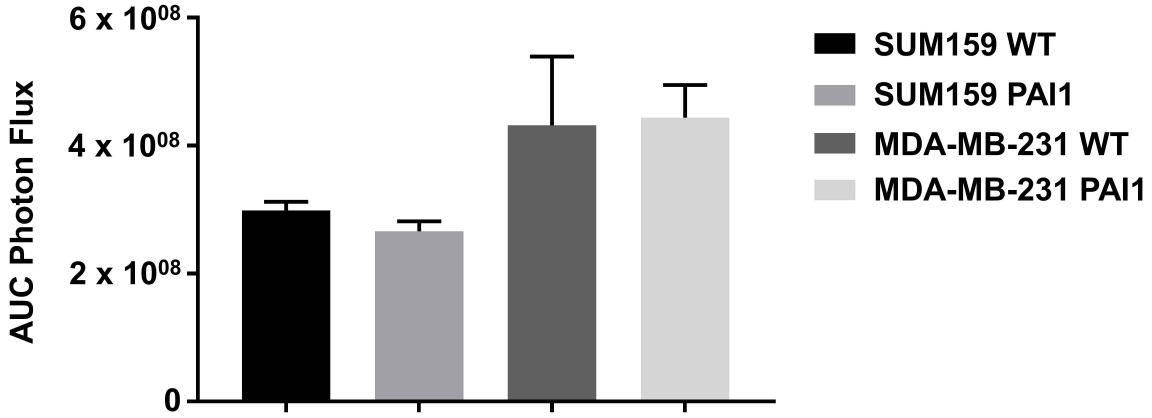

Supplemental Figure S8. PAI1 effects on sphere formation and *in vitro* proliferation. Top. Sphere formation frequency for SUM159 WT and PAI1 cells. Graphs show mean + SD (n = 3000 wells). *** refers to $p < 0.001$. **Bottom.** Area-under-the-curve photon flux for cell growth of SUM159 and MDA-MB-231 WT and PAI1 cells. Graphs show mean + SD (n = 3).

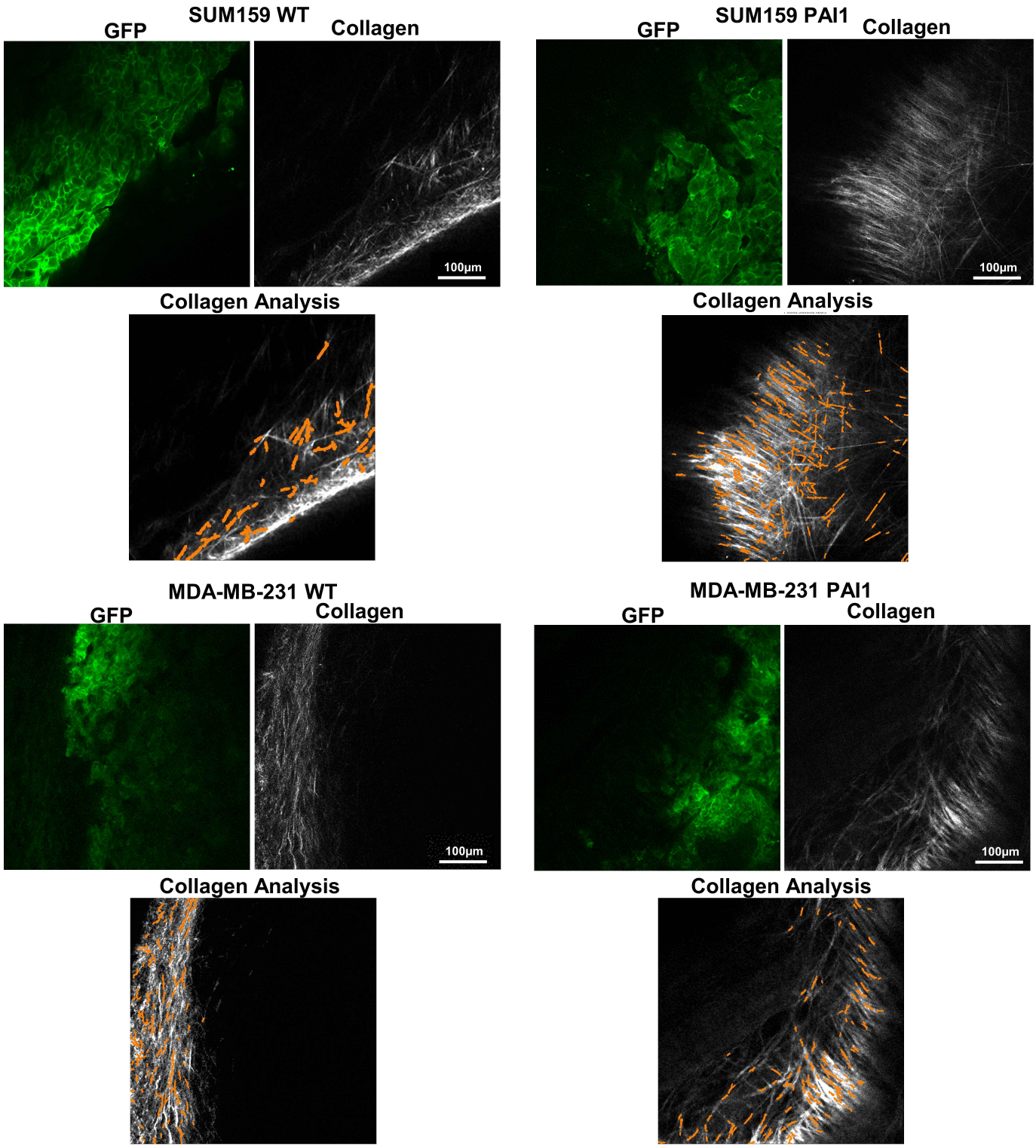

Supplemental Figure S9. PAI1 promotes collagen alignment in mouse orthotopic xenografts. Representative images of orthotopic tumors (green), surrounding collagen (grey), and analysis of the collagen orientation (grey with orange lines) from SUM159 or MDA-MB-231 WT or PAI1 cells that express LifeAct-GFP. We analyzed collagen orientation with custom MATLAB code.